SYNTHESIS, CHARACTERIZATION, ANTIBACTERIAL AND *IN-SILICO* MOLECULAR DOCKING STUDIES OF 2,5-DISUBSTITUTED-1,3,4-OXADIAZOLE DERIVATIVES

K. Santhanalakshmi[1], S. Kalyanasundaram[2], P. Jacquline Rosy[3], S. Muthukumar[4]
[2]Department of chemistry, Poompuhar College (Autonomous), Melaiyur, India
Department of chemistry, I.F.E.T College of Engineering, Gangarampalayam, Villupuram, India

Abstract

We report the ultrasonic synthesis and biological assessment of 1,3,4-oxadiazole substituted 8 derivatives as novel, potential antibacterial agents. The structures of the newly synthesized derivatives were established by the combined practice of IR, ^{1}H NMR and ^{13}C NMR spectrometry. Further these synthesized derivatives were subjected to antibacterial activity against all the selected microbial strains in comparison with ciprofloxacin. Two different docking methods Auto-dock and Glide were performed to compare their suitability for 3,4-oxadiazoles. Interestingly in both the docking programs the ligands have occupied the same binding pocket confirming the selection of active site. Auto-dock yielded better results than Glide for 4a-h whereas the performance of Glide was better in case of 4a-h.

KEY WORDS: Antibacterial, oxadiazole, Molecular Docking, Zone of Inhibition.

1. INTRODUCTION

During the past decades, the human population affected with life threatening infectious diseases caused by multidrug resistant Gram-positive and Gram-negative pathogen bacteria increased to an alarming level around the world. Due to this reason, it is imperative to design and develop new antibacterial or antifungal agents with novel chemical structure preferably having different modes of action rather than analogues of the existing ones. Rational development of antimicrobials mainly relies on development of new compounds against specific targets. 1,3,4-Oxadiazoles have attracted interest in medicinal chemistry as surrogates of carboxylic acids, esters, and carboxamides[1-4]**.** As evident from the literature, in recent years a significant portion of research work in heterocyclic chemistry has been devoted to 1,3,4-oxadiazole containing different aryl groups as substituent. 1,3,4- Oxadiazole is a heterocyclic compound containing an oxygen atom and two nitrogen atoms in a five-membered ring. The ability of 1,3,4-oxadiazole heterocyclic compounds to undergo various chemical reactions has made them important for molecule planning because of their privileged structure, which has enormous biological potential.

The 1,3,4-oxadiazole derivatives have been found to exhibit diverse biological activities such as antimicrobial, anti-HIV[5], antitubercular[6], antimalarial[7], analgesic[8], anti-inflammatory[9], anticonvulsant[10], hypoglycemic[11] and other biological properties such as genotoxic studies[12] and lipid peroxidation inhibitor[13]**.** Used extensively in the symptomatic treatment of rheumatic fever, arthritis[14] (rheumatoid, osteo and Jaundice arthritis), myocardial infarctions and management of primary dysmenorrheal[15].

Substituted 1,3,4-oxadiazoles are of considerable pharmaceutical interest, which was documented by a steadily increasing number of publications and patents. Generally, 2,5-disubstituted-1,3,4-oxadiazole derivatives tend to be stable, particularly 2,5-diaryl-1,3,4-oxadiazoles are more stable than the corresponding 2,5-dialkyl derivatives. Due to the appealing biological activity of 2,5-disubstituted 1,3,4 oxadiazole, an extensive concentration has been focused on this group. For instance, 2-

amino-1,3,4-oxadiazoles act as muscle relaxants[16] and show antimitotic activity. Antihepatitis[17] and antidiarrheal activity[18] of some new 1,3,4-oxadiazoles was also reported.

Apart from these biological activities, 1,3,4-oxadiazole derivatives were found to have some material applications in the field of liquid crystals and photosensitizer. Number of drugs available in the market such as tiodazosin, nosapidil, furamizole are 1,3,4-oxadiazole derivatives. Two examples of compounds containing the 1,3,4-oxadiazole unit currently used in clinical medicine are: Raltegravir® an antiretroviral drug[19] and Zibotentan® an anticancer agent[20]. Ultrasound-assisted organic synthesis is used as a modern and eco-friendly technique that is being used to accelerate organic synthesis. The effect of ultrasound during organic reaction is due to cavitation. The rarefaction-compression cycle in activation process, which involves the separation of molecules of liquids and then the collapse of the bubbles, provides strong impulsions that generate short-lived regions with high temperature and pressure. Such localized hot spots can be thought of as micro reactors in which the sound energy is converted into beneficial chemical form.

Gyrases are DNA topology modifying enzymes that are widely present in prokaryotes[21] These are bacterial type II topoisomerases, which are involved in catalysing reactions such as DNA supercoiling /relaxation, catenation / decatenation and knotting/unknotting[22]. The core protein is of two subunits namely A and B. The subunit A consists of two domains N-terminal breakage and reunion domain and carboxy terminal domain (CTD). The subunit B has ATP hydrolysis domain followed by the Toprim domain. Each domain is found to have a unique role in maintenance of DNA topology. Hence each of the subunit and their respective domain remain an attractive target in development of various antimicrobials.

In the current study the binding mechanism of DNA gyrase with the above mentioned ligands was studied through molecular docking. Two different docking tools, AutoDock and Glide, were used to identify which docking method works better with the target proteins and lipids. The binding of DNA gyrase with the above mentioned ligands was performed *in-silico* analysis. Here we present synthesis, characterization and antibacterial and briefly present results from the docking and screening experiments.

2. MATERIALS AND METHODS.

All the chemicals and solvents used were of AR grade obtained from Sigma Aldrich, Lobachemie (India). Melting points of the synthesized compounds were determined in open-glass on a Staurt-SMP10 melting point apparatus and recorded in ˚0 C without correction. The purity of the compounds was ascertained by thin layer chromatography on silica gel coated aluminum plates (Merck) as adsorbent and UV light as visualizing agent. Synthesized compounds were recrystallised using ethanol as solvent. IR spectra were recorded on SHIMADZU FT-IR spectrometer using KBr pellet technique. ^{1}H-NMR and ^{13}C-NMR spectra were recorded on BRUKER-400 spectrometer operating at 400 MHz using TMS as internal standard in DMSO (chemical shifts in ppm). Protein Structure Preparation The X-ray crystal structures DNA gyrase (PDB: 3U2D) retrieved from the Research Collaboratory for Structural Bioinformatics (RCSB) Protein Data Bank (Figure 1) was used in this study. Water molecules of crystallization were detached from the composite and the protein was optimized for docking using the protein preparation and refinement utility provided by Schrödinger LLC. Partial atomic charges were assigned according to the OPLS-AA force field.

3. MOLECULAR DOCKING STUDIES

3.1. DNA gyrase inhibitor

Crystal structures of the protein complex used in this study were obtained from the the protein data bank (www.rcsb.org/pdb). PDB code: 3U2D[23]

3.2. Docking Studies

The take a look at set of complexes described above was used in the evaluation. DNA gyrase was docked back into the corresponding binding site. In order to get accurate results, all the docking experiments were performed with the default parameters. Docking with was performed on a Autodock 4.2 and Molecular docking server with an Intel Pentium D process or (3.0 GHz) and 4 GB of R A M was run on windows 7. The following

paragraphs describe the search algorithm and scoring methods used in the three programs. For each program, details of the calculations performed in this study are provided.

3.3. Auto Dock 4.2

For AutoDock 4.2, ligand molecules were drawn in ChemBioDraw Ultra 12.0 and converted to their three-dimensional structures in Chem Bio3D Ultra 12.0 and saved as in pdb format. The prepared ligands were used as input files for AutoDock 4.2 in the next step. Lamarckian genetic algorithm method was employed for docking simulations. The standard docking procedure was used for a rigid protein and a flexible ligand whose torsion angles were identified (for 10 independent runs per ligand). A grid of 60, 60, and 60 points in x, y, and z directions was built with a grid spacing of 0.375 A˚ and a distance dependent function of the dielectric constant were used for the calculation of the energetic map. The default settings were used for all other parameters. At the end of docking, the best poses were analyzed for hydrogen bonding/π–π interactions and root mean square deviation (RMSD) calculations using Discovery Studio Visualizer 4.2 (Accelrys Software Inc.) and Pymol (The PyMOL Molecular Graphics System) programs. From the estimated free energy of ligand binding energy, the inhibition constant (Ki) for each ligand was calculated and reproduced in Table 4.

3.4. GLIDE docking

Further, docking studies have also been performed using GLIDE 5.8[24] in standard precision (SP) and extra precision (XP) modes, respectively, as implemented in the Schrödinger Suite. Glide carries out an exhaustive conformational search, augmented by a heuristic screen that rapidly eliminates conformations deemed not to be suitable for binding to a receptor, such as conformations that have long-range internal hydrogen bonds. In SP and XP both dockings, the receptor was kept rigid while ligands were treated as flexible, which enables to dock the ligand at the receptor's binding site to generate multiple poses of the receptor–ligand complex, each including unique structural conformations of the ligands to fit in the binding site of receptor and ranks them by Glide score (G-score) to find the best structure of the docked complex. The G-score takes into account a number of parameters like hydrogen bonds (H-bond), hydrophobic contacts (Lipo), van der Waals (vdW), columbic (Coul), polar interactions in the binding site (Site), metal binding term (Metal) and penalty for buried polar group (BuryP) & freezing rotatable bonds (RotB)

4. ANTIBACTERIAL ACTIVITY

The newly prepared compounds were screened for their antibacterial activity against Escherichia coli, Staphylococcus aureus, Pseudomonas aeruginosa Streptococcus pyogenes and Bacillus Subtilis bacterial strains by disc-diffusion method [25-26]. A standard was introduced on to the surface of sterile agar plates, and a sterile glass spreader was used for even distribution of the inoculum. The discs measuring 6.25 mm in diameter were prepared from Whatman no. 1 filter paper and sterilized by dry heat at 140 °C for 1 h. The sterile discs previously soaked with the test compound solution in DMSO of specific concentration 100 µg/disc were carefully placed on the agar culture plates. The plates were incubated at 37 °C and the diameter of the growth inhibition zones were measured after 24h. The plates were inverted and incubated for 24 h at 37 °C. Ciprofloxacin was used as a standard drug. Inhibition zones were measured and compared with the Ciprofloxacin.

5. SYNTHESIS

5.1 Synthesis of ester[27]: In a 250 ml round bottom flask, a mixture of carboxylic acid (0.1mol), ethanol (60 ml) and conc. H_2SO_4 (1.4 ml) were irradiated for 1 hour on a ultrasonic cleaning bath. The solution was cooled and poured slowly with stirring on to 200 g of crushed ice. Sufficient ammonia solution was added to render the resulting solution alkaline, generally some ester separates as oil but most of it remains dissolved in the alkaline solution. The solution was extracted five times with ether (25 ml) the combined ethereal extract was dried with anhydrous $MgSO_4$. Ether was removed by evaporation on a water bath and the residue was collected. Physical data of ester was noted; Yield 76%.The Synthetic procedure is shown in scheme 1.

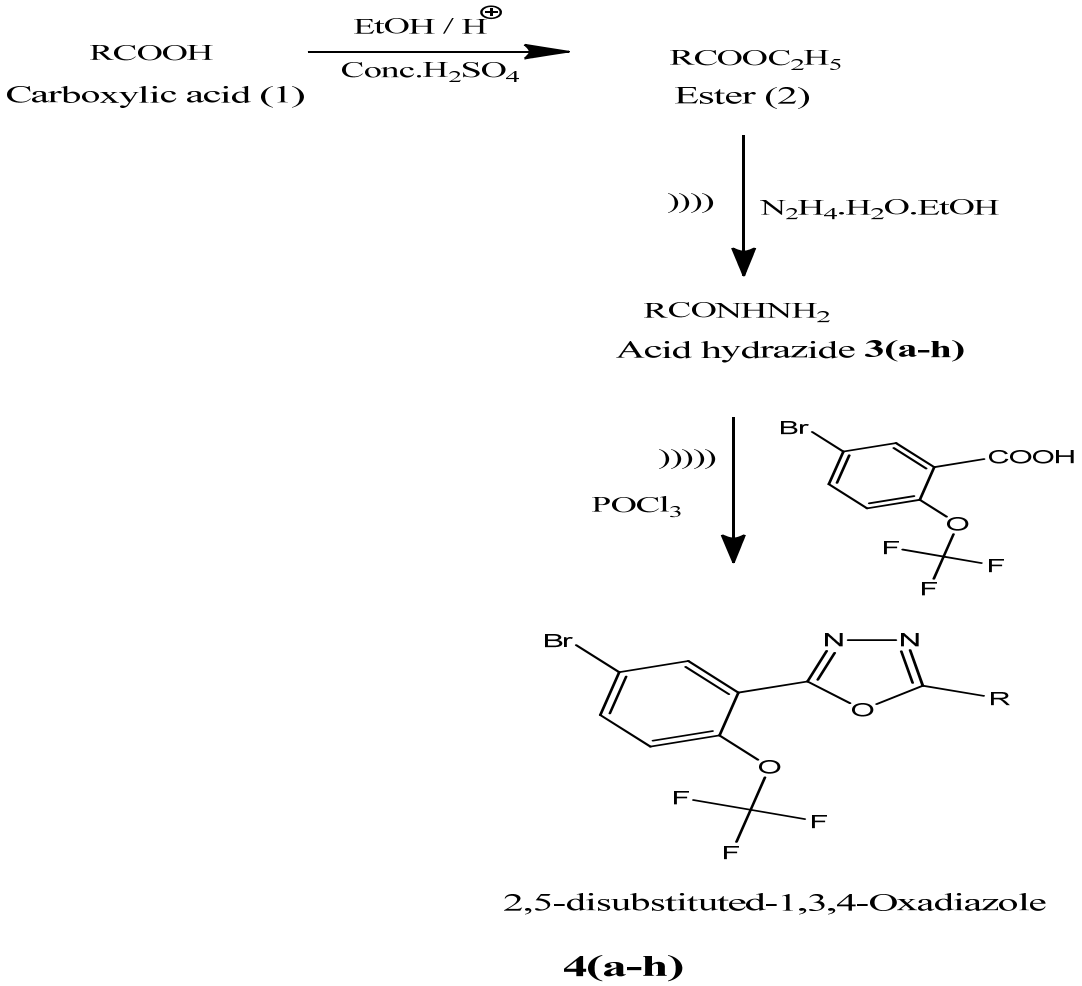

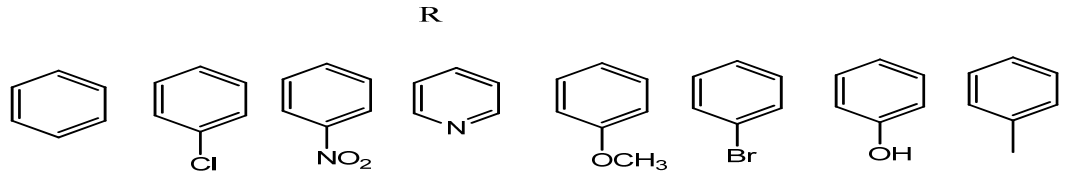

Scheme 1

5.2 Synthesis of acid hydrazide 3(a-h)[27]: A mixture of ester and hydrazine hydrate in 1:1 portion and ethanol (30 ml) were taken in a round bottom flask and irradiated for 30 min. Excess of ethanol was removed by distillation. On cooling the product, acid hydrazide separates out. It was filtered and collected. Recrystallization was carried out with ethanol and physical data was noted. Yield 65%. The physical properties of synthesized derivatives 3(a-h) are shown in Table 1.

5.3 Synthesis of 2,5-disubstituted-1,3,4-Oxadiazole 4(a-h). A mixture of acid hydrazide (0.01 mol) and 5-bromo-2-(trifluoromethoxy)benzoic acid (0.01mol) in $POCl_3$ (5ml) was irradiated on ultrasonic cleaning bath for 2 hrs. The reaction mixture was cooled and poured into crushed ice. It was neutralized with sodium bicarbonate solution and the resulting solid was filtered, dried and washed with water and recrystallized from ethanol to give 2,5-disubstituted-1,3,4-Oxadiazole 4(a-h). The physical properties of synthesized derivatives 4(a-h) are shown in Table 2.

Table 1: Physical properties and IR Spectral Data of Synthesized Hydrazides 3(a-h)

Compound	R	Molecular formula	M.Pt (˚C)	M.Formula	Physical state	IR Frequency
3a	C_6H_5	$C_7H_8N_2O$	110	136	White powder	3032 cm^{-1} (C-H Ar str); 1622 cm^{-1}(C=O str); 3296, 3215 ($NHNH_2$ str); 985 cm^{-1} (N-N str).
3b	C_6H_5Cl	$C_7H_7ClN_2O$	162	170	White powder	3016 cm^{-1} (C-H Ar str); 1645 cm^{-1} (C=O str); 3302, 3209 cm^{-1} ($NHNH_2$ str); 727 cm^{-1} (C-Cl str); 987 cm^{-1} (N-N str).
3c	$C_6H_5NO_2$	$C_7H_7N_3O_3$	215	181	Pale Yellow powder	3070 cm^{-1} (C-H Ar str); 1662 cm^{-1} (C=O str); 3296, 3180 cm^{-1} ($NHNH_2$ str); 1525 cm^{-1} (NO_2 str); 1055 cm^{-1} (N-N str).
3d	C_5H_5N	$C_6H_7N_3O$	170	137	White powder	3064 cm^{-1} (C-H Ar str); 1649 cm^{-1} (C=O str); 3305, 3178 cm^{-1} ($NHNH_2$ str); 1045 cm^{-1} (N-N str).
3e	$C_6H_5OCH_3$	$C_8H_{10}N_2O_2$	135	166	White powder	3043 cm^{-1} (C-H Ar str); 2933 cm^{-1} (C-H Aliphatic str); 1612 cm^{-1} (C=O str); 3381, 3253 cm^{-1} ($NHNH_2$ str); 1031 cm^{-1} (N-N str).
3f	C_6H_5Br	$C_7H_7BrN_2O$	164	215	White powder	3016 cm^{-1} (C-H Ar str); 1651 cm^{-1} (C=O str); 3415, 3305 cm^{-1} ($NHNH_2$ str); 1006 cm^{-1} (N-N str).
3g	C_6H_5OH	$C_7H_8N_2O_2$	260	152	White powder	3068 cm^{-1} (C-H Ar str); 1629 cm^{-1} (C=O str); 3309, 3197 cm^{-1} ($NHNH_2$ str); 1056 cm^{-1} (N-N str).
3h	$C_6H_5CH_3$	$C_8H_{10}N_2O$	115	150	White powder	3053 cm^{-1} (C-H Ar str); 2953 cm^{-1} (C-H Aliphatic str); 1625 cm^{-1} (C=O str); 3331, 3207 cm^{-1} ($NHNH_2$ str); 1033 cm^{-1} (N-N str).

Table-2: Physical Data of the Synthesized Compounds 4(a-h):

Compound	R	Molecular Formula	M.Pt (˚C)	Yield(%)	Physical state
4a	C_6H_5	$C_{15}H_8BrF_3N_2O_2$	193-195	69	Pale Yellow powder
4b	C_6H_5Cl	$C_{15}H_7BrClF_3N_2O_2$	132-135	72	Pale Yellow powder
4c	$C_6H_5NO_2$	$C_{15}H_7BrF_3N_3O_4$	152-155	65	Dark brown powder
4d	C_5H_5N	$C_{14}H_7BrF_3N_3O_2$	146-147	66	Pale Yellow powder
4e	$C_6H_5OCH_3$	$C_{16}H_{10}BrF_3N_2O_3$	124-126	75	Pale Yellow powder
4f	C_6H_5Br	$C_{15}H_7Br_2F_3N_2O_2$	162-165	63	Pale Yellow powder
4g	C_6H_5OH	$C_{15}H_8BrF_3N_2O_3$	122-124	71	Pale Yellow powder
4h	$C_6H_5CH_3$	$C_{16}H_{10}BrF_3N_2O_2$	116-119	67	Pale Yellow powder

5.4 Analytical data of compounds 4a-h

5.4.1. 2-(5-bromo-2-(trifluoromethoxy) phenyl)-5-phenyl-1,3,4-oxadiazole (4a):

IR (KBr): 3078 cm^{-1} (C-H Ar str); 1598 cm^{-1} (C=N str); 503 cm^{-1} (C-Br str); 1165 cm^{-1} (C-F str); 1080 cm^{-1} (N-N str). ^{1}H-NMR (400 MHz, DMSO-d_6): 7.09-7.93 δ (8H, Aromatic protons); ^{13}C-NMR (400 MHz, DMSO-d_6): 114.02-133.35 δ (Aromatic carbon); 163.11 δ (C of 1,3,4-Oxadiazole ring); 151.66 δ (C-O).

5.4.2. 2-(5-bromo-2- (trifluoromethoxy) phenyl)-5-(4-chlorophenyl)-1,3,4-oxadiazole (4b)

IR (KBr): 3076 cm^{-1} (C-H Ar str); 1602 cm^{-1} (C=N str); 516 cm^{-1} (C-Br str); 1165 cm^{-1} (C-F str); 1062 cm^{-1} (N-N str); 736 cm^{-1} (C-Cl str). ^{1}H-NMR (400 MHz, DMSO-d_6): 6.86-7.44 δ (7H, Aromatic protons); ^{13}C-NMR (400 MHz, DMSO-d_6): 117.16-138.77 δ (Aromatic carbon); 161.72 δ (C of 1,3,4-Oxadiazole ring); 152.18 δ (C-O).

5.4.3.2-(5-bromo-2-(trifluoromethoxy) phenyl)-5-(4-nitrophenyl)-1,3,4-oxadiazole (4c)

IR (KBr): 3066 cm^{-1} (C-H Ar str); 1602 cm^{-1} (C=N str); 505 cm^{-1} (C-Br str); 1166 cm^{-1} (C-F str); 1060 cm^{-1} (N-N str). ^{1}H-NMR (400 MHz, DMSO-d_6): 7.10-7.94 δ (7H, Aromatic protons); ^{13}C-NMR (400 MHz, DMSO-d_6): 114.11-134.58 δ (Aromatic carbon); 166.76 δ (C of 1,3,4-Oxadiazole ring); 152.11 δ (C-O).

5.4.4.4-(5-(5-bromo-2-(trifluoromethoxy) phenyl)-1,3,4-oxadiazol-2-yl)pyridine (4d)

IR (KBr): 3064 cm^{-1} (C-H Ar str); 1612 cm^{-1} (C=N str); 513 cm^{-1} (C-Br str); 1161 cm^{-1} (C-F str); 1060 cm^{-1} (N-N str). ^{1}H-NMR (400 MHz, DMSO-d_6): 7.06-7.90 δ (7H, Aromatic protons); ^{13}C-NMR (400 MHz, DMSO-d_6): 119.03-134.86 δ (Aromatic carbon); 156.95 δ (C of 1,3,4-Oxadiazole ring); 156.08 δ (C-O).

5.4.5.2-(5-bromo-2-(trifluoromethoxy) phenyl)-5-(4-methoxyphenyl)-1,3,4-oxadiazole (4e) IR (KBr): 3080 cm^{-1} (C-H Ar str); 2941 cm^{-1} (C-H Aliphatic str); 1579 cm^{-1} (C=N str); 536 cm^{-1} (C-Br str); 1166 cm^{-1} (C-F str); 1064 cm^{-1} (N-N str). ^{1}H-NMR (400 MHz, DMSO-d_6): 7.04-7.91 δ (7H, Aromatic protons); 3.82 δ (3H, OCH_3 group). ^{13}C-NMR (400 MHz, DMSO-d_6): 113.65-139.95 δ (Aromatic carbon); 166.27 δ (C of 1, 3, 4-Oxadiazole ring); 55.32 δ (OCH_3 group); 151.65 δ (C-O).

5.4.6.2-(5-bromo-2-(trifluoromethoxy) phenyl)-5-(4-bromophenyl)-1,3,4-oxadiazole (4f)

IR (KBr): 3070 cm^{-1} (C-H Ar str); 1606 cm^{-1} (C=N str); 528 cm^{-1} (C-Br str); 1062 cm^{-1} (C-F str); 1178 cm^{-1} (N-N str). ^{1}H-NMR (400 MHz, DMSO-d_6): 7.04-7.91 δ (7H, Aromatic protons); ^{13}C-NMR (400 MHz, DMSO-d_6): 114.56-135.88 δ (Aromatic carbon); 166.76 δ (C of 1,3,4-Oxadiazole ring); 152.15 δ (C-O).

5.4.7.4-(5-(5-bromo-2-(trifluoromethoxy) phenyl)-1,3,4-oxadiazol-2-yl)phenol (4g)

R (KBr): 3083 cm^{-1} (C-H Ar str); 1598 cm^{-1} (C=N str); 503 cm^{-1} (C-Br str); 1168 cm^{-1} (C-F str); 1062 cm^{-1} (N-N str). ^{1}H-NMR (400 MHz, DMSO-d_6): 7.03-7.84 δ (7H, Aromatic protons); 10.12 δ (1H, OH group) ^{13}C-NMR (400 MHz, DMSO-d_6): 111.94-136.36 δ (Aromatic carbon); 165.31 δ (C of 1,3,4-Oxadiazole ring); 158.36 δ (C-O).

5.4.8.2-(5-bromo-2-(trifluoromethoxy) phenyl)-5-*p*-tolyl-1,3,4-oxadiazole (4h)

IR (KBr): 3072 cm^{-1} (C-H Ar str); 2945 cm^{-1} (C-H Aliphatic str); 1608 cm^{-1} (C=N str); 495 cm^{-1} (C-Br str); 1168 cm^{-1} (C-F str); 1060 cm^{-1} (N-N str). ^{1}H-NMR (400 MHz, DMSO-d_6): 7.16-7.98 δ (7H, Aromatic protons); 2.49 δ (3H, CH_3 group). ^{13}C-NMR (400 MHz, DMSO-d_6): 117.14-135.90 δ (Aromatic carbon); 164.77 δ (C of 1,3,4-Oxadiazole ring); 26.10 δ (CH_3 group); 152.17 δ (C-O).

6. RESULTS AND DISCUSSION

6.1. Antibacterial Activity

The *in vitro* antibacterial activity of 1,3,4-oxadiazole derivatives were investigated against gram positive organisms (*Staphylococcus aureus, Bacillus subtilisand Streptococcus pyogenes)* and gram negative organisms *(Escherichia coli* and *Pseudomonas aeruginosa).* Results are summarized in Table 3 and zone of inhibitions were shown in Figure 1 and 2 along with standard drug. All analogues, showed comparable antibacterial activity at the dose 100µg/ml against all the tested strains. Results indicate that compounds 4a, 4d and 4e showed maximum activity against Escherichia coli (zone of inhibition=17, 18 and 23 mm at the dose of 100µg/ml) in comparison to other strains used by us. Compounds 4b and 4d Showed maximum activity against *Pseudomonas aeruginosa (*zone of inhibition- 17 and 18 mm at the dose of 100µg/ml) 4b showed maximum activity against *Streptococcus pyogenes* (zone of inhibition=18mm).

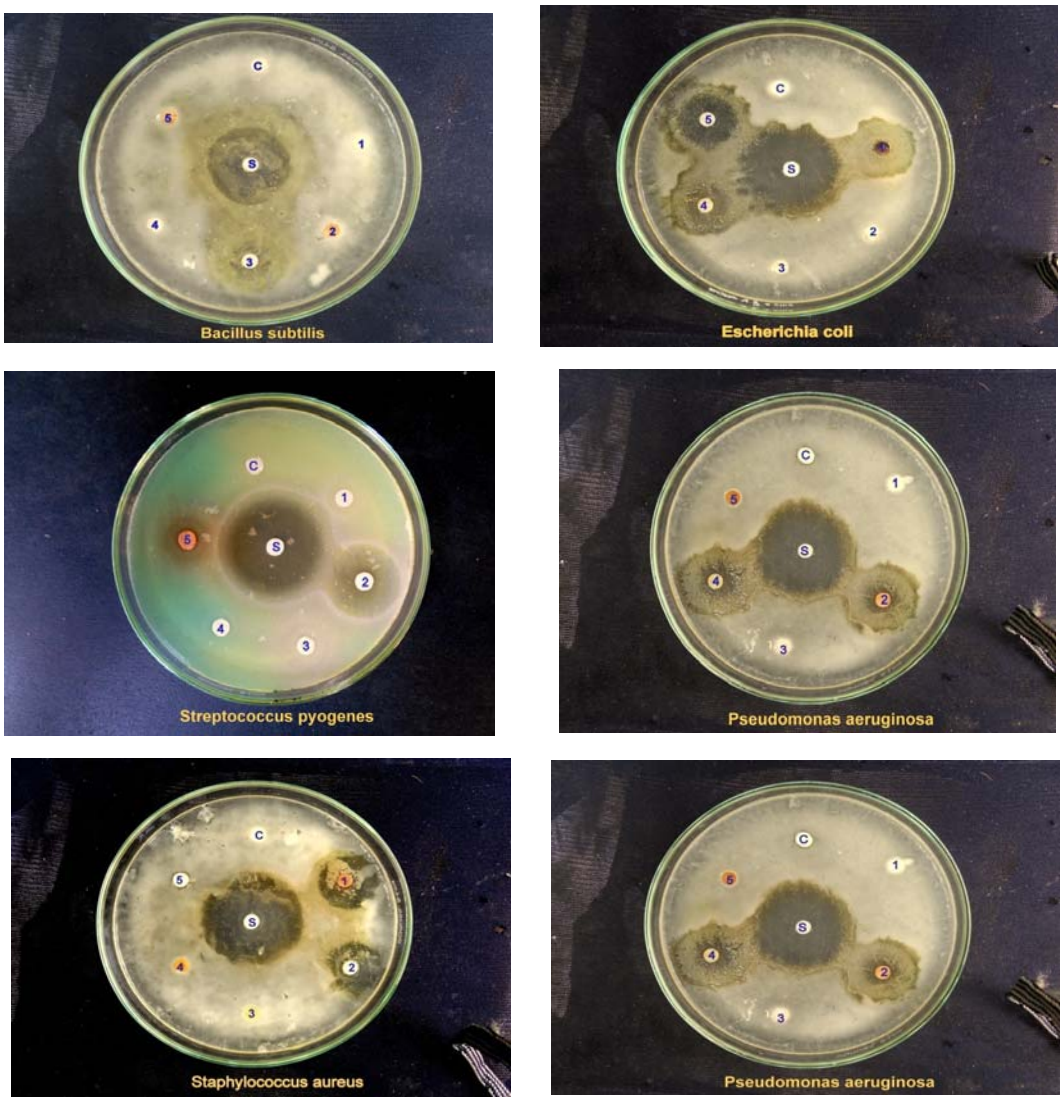

Figure 1: Antibacterial activity of 2,5-disubstituted -1,3,4-oxadiazole derivatives 4(a-e)

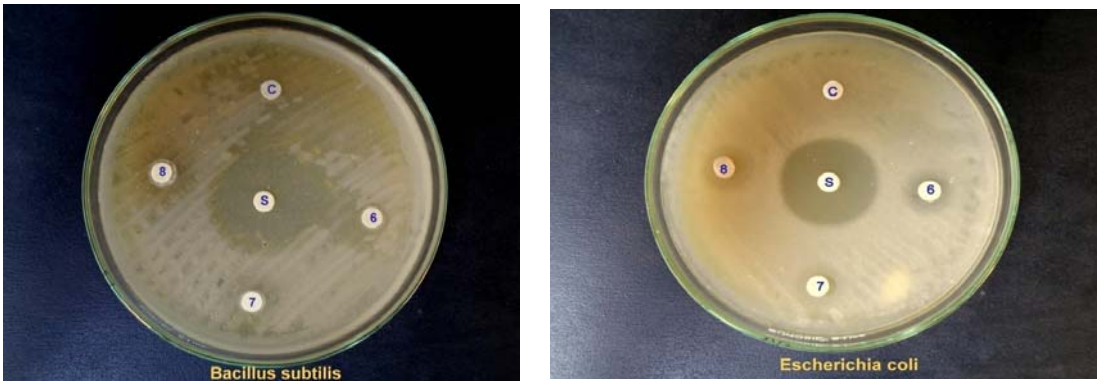

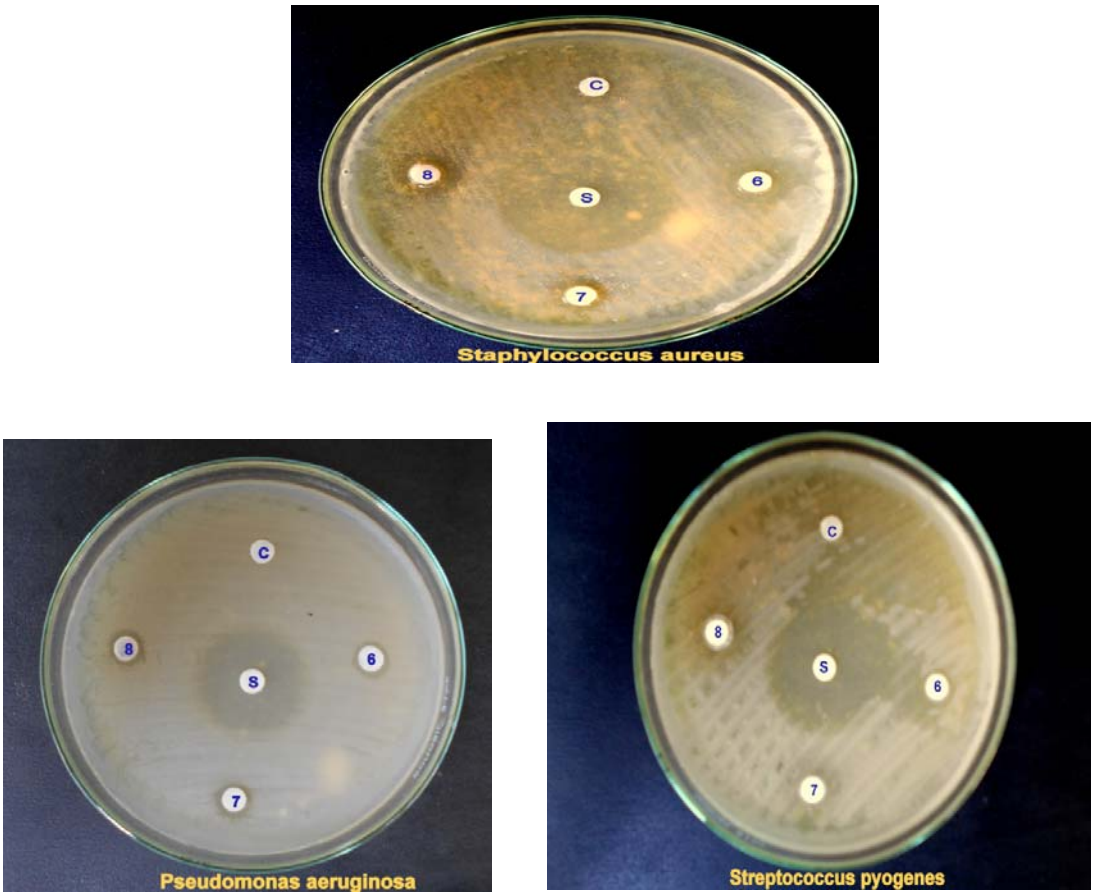

Figure 2: Antibacterial activity of 2,5-disubstituted -1,3,4-oxadiazole derivatives 4(f-

Table 3: Antibacterial activity of synthesized 2,5-disubstituted-1,3,4-oxadiazole derivatives 4(a-h)

S. No.	Bacteria	Standard Antibiotic Disk*	Zone of inhibition mm in diameter							
			1	2	3	4	5	6	7	8
1	*Bacillus subtilis*	24	-	-	16	-	14	11	13	15
2	*Escherichia coli*	30	17	-	-	18	23	13	12	15
3	*Pseudomonas aeruginosa*	31	-	17	-	18	-	11	11	11
4	*Staphylococcus aureus*	30	17	15	-	-	09	14	12	13
5	*Streptococcus pyogenes*	32	12	18	-	-	14	11	-	14

*ciprofloxacin

Table 4 Docking results of **4a-h** with DNA gyrase (PDB code: 3U2D)

S.NO	Binding energy Kca/mol^{-1}	Docking score Kca/mol^{-1}	Vdw_hb_desolv_energy Kca/mol^{-1}	Glide energy Kca/mol^{-1}	Inhibition constant (μm)	Hydrogen bonding		Residues involving interactions		RMSD	
	Auto Dock 4.2		Auto Dock 4.2		Auto Dock 4.2	Auto Dock 4.2	Glide	Auto Dock 4.2	Glide		
4a	-7.42	-4.61	-8.60	-41.54	3.65	2	0	THR A:173 GLY A:85	-	24.444	3.56
4b	-7.83	-4.65	-9.01	-43.08	1.82	2	0	THR A:173 GLY A:85	-	24.53	4.79
4c	-7.87	-4.76	-9.06	-45.19	1.70	4	1	SER B:55 ASP B:81 ILE B:175 ARG B:144	ARG84	24.48	0.13
4d	-6.60	-6.26	-8.08	-38.96	14.57	2	1	GLY B:85 THR B:173	GLY85	24.71	2.39
4e	-7.73	-4.41	-8.94	-43.14	2.17	2	0	THR A:173 GLY A:85	-	24.12	3.61
4f	-8.56	-4.48	-9.71	-43.45	5.3	1	0	THR A:173	-	24.54	0.84
4g	-7.08	-5.08	-8.53	-34.57	6.08	2	1	THR A:173 GLY A:85	ASP81	24.85	0.57
4h	-7.27	-5.20	-8.40	-35.28	4.72	3	0	SER B:55 ASP B:81 ILE B:175		24.53	4.38
	-7.08	-7.63	-7.03	-33.58	6.63	2	2	ASP A:161 ASP B:57	GLU58 SER129	24.10	3.43

6.2. Docking analysis

The molecular docking studies were performed against crystal structure of DNA gyrase and the respective docking scoring functions were given in Table 4 and Figure 3 shows the X-ray crystal structure of protein DNA gyrase (PDB: 3U2D) and Docking images of synthesized 1, 3, 4-Oxadiazole derivatives **4c, 4d** and **4g**.The docking analysis was finished for the ligands with the target protein DNA gyrase by means of docking software GLIDE and the docked images are exposed.

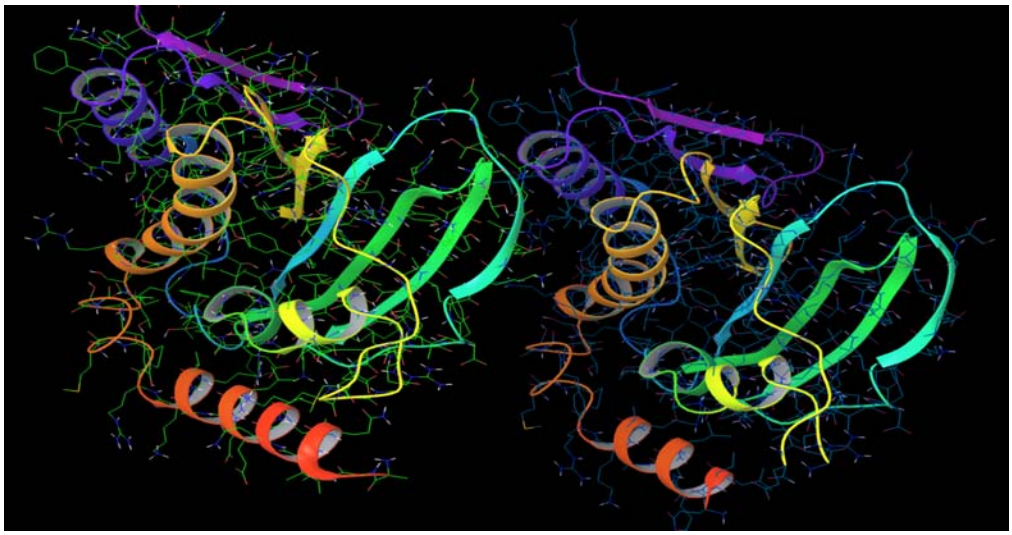

Figure 3: X-ray crystal structure of protein DNA gyrase (PDB: 3U2D)

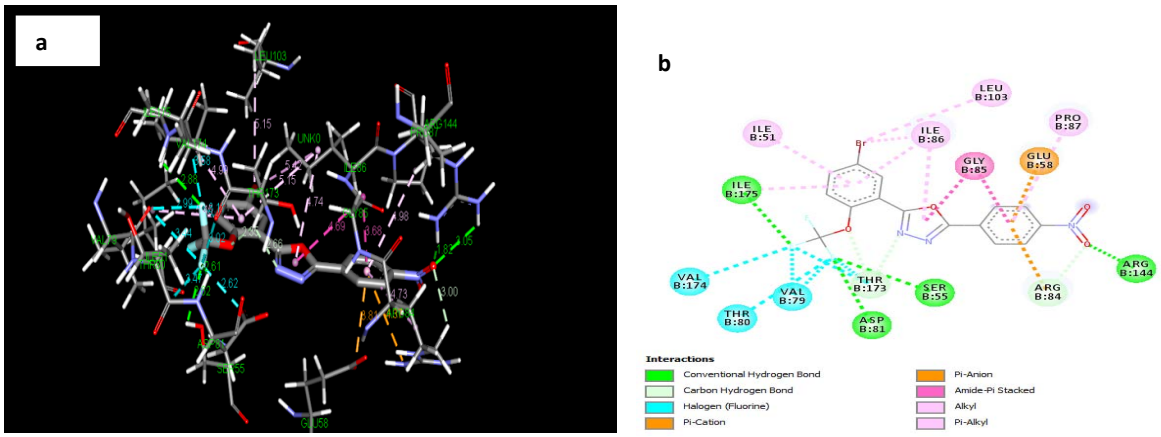

Fig. 4 Docked conformation of most active compound **4f** in auto-dock 4.2 anlysis [(**a**) Binding interaction (**b**) 2-D View]

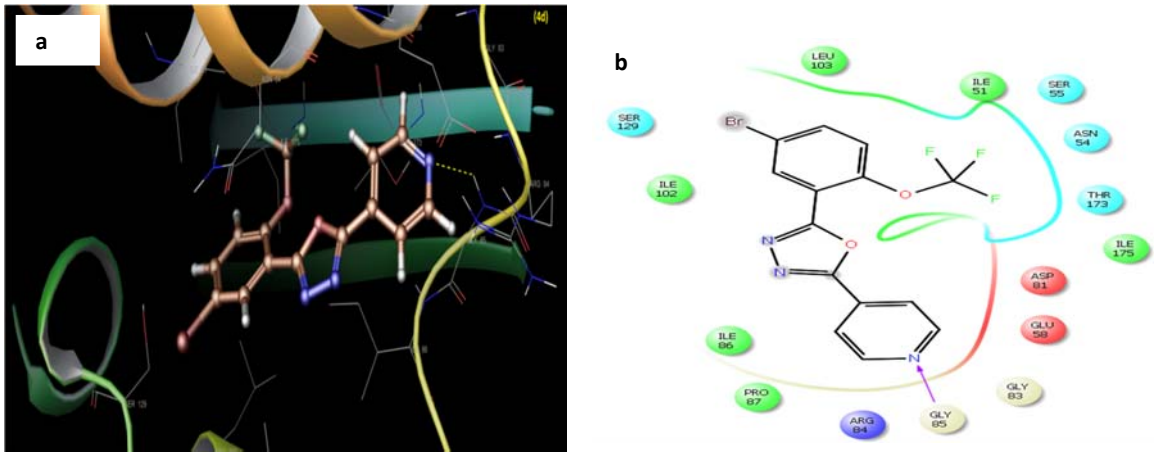

Fig. 5 Docked conformation of most active compound **4d** in Glide anlysis [(**a**) Binding interaction (**b**) 2-D View]

6.2.1. Auto-dock 4.2. analysis

The Conformational search and docking studies using Auto-Dock4.2 suggest that electronic interaction plays an important role in ligand–channel interaction. The results are shown in Table 4. For molecules **4f, 4c, 4b, 4a, 4g** and **4e** have better binding energy values. Molecule **4d** has the minimum binding energy of −6.60 kcal/mol. It is also clear that the standard drug that showed the least binding energies than the designed candidate. Molecule **4f** has higher binding energy. It has been reported that **4f** forms a covalent interaction with the side chain THR A: 173. These *in-silico* findings are well supported by results of in-vitro antibacterial activity. The binding pattern of **4f** with DNA gyrase was depicted in Figs 4 and clearly raveled that the compound **4f** showed major bonding interactions with THR A:173. The standard drug *Ciprofloxin* showed binding interactions with Asp 161 and Asp 57 with binding energy -7.08 (Table 4) which is close to docking score of compound **4g.**

6.2.2. Glide analysis

The structures docked by GLIDE are generally ranked according to the GLIDE Scoring Function (more negative). The scoring function of GLIDE docking agenda is accessible in the G-score form. The majority straightforward technique of evaluating the accurateness of a docking procedure is to establish how closely the lowest energy pose (binding conformation) predicted by the object scoring function. The docking score using GLIDE wide-ranging from -4.41 to – 6.27 Kca/mol^{-1} against DNA gyrase. The GLIDE Score for the standard ciprofloxacin, docked with DNA gyrase was -7.63 Kca/mol^{-1}. Generally for low GLIDE score, good ligand affinity to the receptor may possibly be expected. Compound **4d** showed the finest inhibition for the DNA gyrase with -6.27 Kca/mol^{-1} glide score compared to all other ligands considered for docking. However, the docking energy of molecule **4a** is comparable to that of molecules **4b, 4c, 4e** and **4f**. Since the molecules **4b, 4c, 4e** and **4f** have similar moieties with a small difference in their phenyl substituents, it has been observed that pyidine analogue **4d** is more suitable for binding than phenyl analogue. The synthesized oxadiazoles derivatives are shown to be exhibit good binding its binding sites of DNA Gyrace by interacting with ARG-84, ASP-81 and GLY-85.

5. CONCLUSIONS

A series of 2,5-disubstituted -1,3,4-oxadiazoles 4(a-h) derivatives were synthesized by reaction of substituted acid hydrazides and 5-bromo-2-(trifluoromethoxy)benzoic acid. The chemical structures of the newly synthesized compounds were characterized by IR, ^{1}HNMR, and ^{13}C NMR spectroscopy. The title compounds were evaluated for antibacterial activity by disc diffusion method against various bacterial strains. All the synthesized compounds were found to moderate active against bacteria strains. We have summarized the recent applications of ultrasound-promoted synthetic methodologies for preparation 1,3,4-oxadiazole derivatives. In comparison to conventional methods, ultrasound irradiation provides several advantages such as enhanced reaction rates, selectivity, shorter reaction times, higher yields and environment friendly technique. Docking study was also performed with Auto-dock 4.2 and Glide analysis in order to check interaction of synthesized compounds with the target DNA gyrase and compare theoretical results with experimental values. Form the results in Table 4, we conclude Auto-dock yielded better results than Glide for **4a-h** whereas the performance of Glide was better in case of **4a-h**. Thus it confirms that, the experimental values moderately agree with theoretical values, which suggest that the parameters for docking simulation are optimum in reproducing experimental orientation of these compounds. It may be a good start to use a novel class of biologically active compounds **4a-h** in treating bacterial disorders.

7. REFERENCES:

1. Ramazani, A.; Rezaei, A. *Org. Lett*. 2010, 12 2852-2855.
2. Holla, B. S.; Gonsalves, R.; Shenoy, S. Eur. *J. Med. Chem*. 2000, 35, 267-271.
3. Chen, Q.; Zhu, X. –H.; Jiang, L. –L.; Liu, Z. –M.; Yang, G. –F. Eur. *J. Med. Chem.* 2008, 43, 595-603
4. Amir, M.; Shikha, K. Eur. *J. Med. Chem*. 2004, 39, 535-545
5. A.A. El-Emam, O.A. Al-Deeb, M. Al-Omar, J. Lehmann, *Bioorg. Med. Chem*. 12 (2004) 5107-5113.
6 S.G. Kucukguzel, E.E. Oruc, S. Rollas, F. Sahin, A. Ozbek, *Eur. J. Med. Chem*. 37 (3) (2002) 197-206.

7 P.R. Kagthara, N.S. Shah, R.K. Doshi, H.H. Parekh, *Indian J. Chem*. 38B (1999) 572-576.

8 M. Akhter, A. Husain, B. Azad, M. Ajmal, *Eur. J. Med. Chem*. 44 (2009) 2372-2378.

9 P.C. Unangast, G.P. Shrum, D.T. Conner, C.D. Dyer, D.J. Schrier, *J. Med. Chem*. 35 (1992) 3691-3698.

10 M.S.Y. Khan, R.M. Khan, S. Drabu, *Indian J. Heterocycl. Chem*. 11 (2001) 119-122.

11 J.B. O'Neal, H. Rosen, P.B. Russell, A.C. Adams, A. Blumenthal, *J. Med. Chem*. 5 (3) (1962) 61 626.

12 A.O. Maslat, M. Abussaud, H. Tashtoush, M. Al-Talib, *Pharmacology* 54 (2002) 55-59.

13 A.A. Farghaly, A.A. Bekhit, J.Y. Park, *Arch. Pharm. (Weinheim*) 333 (2000) 53-57.

14 Song Cao, Xu Hong Qian, Gonghua Song, Bing Chai, Zhisheng Jiang, *J. Agric. Food Chem*. 15 (2003) 152-155.

15 S.N. Pandeya, A Text Book of Medicinal Chemistry. *S.G. Publisher*, Varanasi, 2001, 353.

16 Yale, H. L.; Losee, K. *J. Med. Chem*. 1966, 9, 478–483.

17 Tan, T. M. C.; Chen, Y.; Kong, K. H.; Bai, J.; Li, Y.; Lim, S. G.; Ang, T. H.; Lam, Y. *Antiviral Res.* 2006, 71, 7–14.

18 Adelstein, G. W.; Yen, C. H.; Dajani, E. Z.; Bianchi, R. G. *J. Med. Chem. 1976, 19, 1221-1225.*

19 Savarino, A. *Drugs* 2006, 15, 1507–1522.

20 James, N.D.; Growcott, J.W. Zibotentan. *Drugs Future* 2009, 34, 624–633.

21 K. Mdluli, Z. Ma, *Mycobacterium tuberculosis* DNA gyrase as a target for drug discovery. Infect. Disord, Drug Targets., **7**(2), 1-10, (2007).

22 G. Witz, A. Stasiak, DNA supercoiling and its role in DNA decatenation and unknotting. Nucleic Acids Res., **38**(7), 2119-2133, (2010).

23 GM. Morris, DS. Goodsell, RS. Halliday, R. Huey, WE. Hart, RK. Belew, AJ. Olson, J. Comp. Chem., 19 (1998) 1639–1662.

24 Glide version 5.8 Schrödinger, LLC, New York (2012)

25 Andurmila Joshi, Manoj Kumar Gadhwal, Swati Patil, Priscilla D Mello. Int J Pharm Pharm Sci, 2013; 5(2):76-81.

26 Collins, A.H., Microbiological Methods, second ed. Butterworth, London, 1976.

27 K. K. Jha, Abdul Samad, Kumar Yatendra, Shaharyar Mohd., Khosa R. L., Jain Jainendra, Kumar Vikash, Singh Priyanka, European Journal of Medicinal Chemistry; 2010, 45: 4963-4967.

28 Dinesh Mehta, Rina Das, Kamal Dua: *International Journal of Chemical sciences* 2009; 7(1):225-234.